



Hillslope threshold response to rainfall: (1) A field based forensic approach

Chris B. Graham^{a,*}, Ross A. Woods^b, Jeffrey J. McDonnell^{c,d}

^a Department of Crop and Soil Sciences, The Pennsylvania State University, University Park, PA, United States

^b National Institute of Water and Atmospheric Research, Christchurch, New Zealand

^c Department of Forest Engineering, Resources and Management, Oregon State University, Corvallis, OR, United States

^d University of Aberdeen, School of Geosciences, Aberdeen, Scotland, United Kingdom

ARTICLE INFO

Keywords:

Hillslope hydrology
Runoff generation
Tracers
Destructive sampling
Preferential flow
Subsurface flow

SUMMARY

Hillslope threshold response to storm rainfall is poorly understood. Basic questions regarding the type, location, and flow dynamics of lateral, subsurface flow remain unanswered, even at our most intensively studied field sites. Here we apply a forensic approach where we combined irrigation and excavation experiments at the well studied Maimai hillslope to determine the typology and morphology of the primary lateral subsurface flowpaths, and the control of bedrock permeability and topography on these flowpaths. The experiments showed that downslope flow is concentrated at the soil bedrock interface, with flowpath locations controlled by small features in the bedrock topography. Lateral subsurface flow is characterized by high velocities, several orders of magnitude greater than predicted by Darcy's Law using measured hydraulic conductivities at the site. We found the bedrock to be moderately permeable, and showed that vertical percolation of water into the bedrock is a potentially large component of the hillslope water balance. Our results suggest that it is the properties of the bedrock (topography and permeability) that control subsurface flow at Maimai, and the soil profile plays a less significant role than previously thought. A companion paper incorporates these findings into a conceptual model of hydrological processes at the site to explore the generalities of whole-hillslope threshold response to storm rainfall.

© 2010 Elsevier B.V. All rights reserved.

Introduction

Hillslopes are fundamental units of the hydrologic landscape and the main filter for water and solute transport from the atmosphere to the stream. In forested regions of the world, quick lateral subsurface stormflow (often called interflow or throughflow) is the primary mechanism for stormflow generation in headwater catchments (Hursh, 1944). Much of the progress in identifying the different manifestations of subsurface stormflow behaviors was made in the 1960s and 1970s (Hewlett and Hibbert, 1967; Mosley, 1979; Whipkey, 1965). More recent work has tempered community excitement about these discoveries by revealing the staggering complexity, heterogeneity and uniqueness of hillslope drainage systems (McDonnell et al., 2007) and the enormous range of scales of processes imposed by climate, geology and vegetation that control hillslope response (Sidle et al., 2007; Sivapalan, 2003; Zehe et al., 2007).

While determining slope-specific processes remains daunting, one common denominator in hillslope response to rainfall is the

often-observed threshold relationship between total storm precipitation and lateral subsurface stormflow (Fig. 1). This threshold relationship is an emergent property at the hillslope scale – a property that subsumes much of the sub-grid complexity at the plot scale (e.g. Lehmann et al., 2007). While threshold relationships between storm rainfall and hillslope-scale runoff have been shown now in several environments around the world based on hillslope trenchflow recording (Buttle and McDonald, 2002; Hutchinson and Moore, 2000; Mosley, 1979; Spence and Woo, 2002; Tani, 1997; Uchida et al., 1999, 2005) the physical cause of these thresholds has been difficult to generalize given the challenge of making hillslope-scale measurements. Recently, (Tromp-van Meerveld and McDonnell, 2006b) proposed “fill and spill” as a conceptual framework to explain the whole-slope precipitation threshold for lateral subsurface stormflow. The fill and spill theory states that connectivity of patches of (transient) subsurface saturation (at the interface between the soil and an impeding layer) is a necessary pre-condition for significant hillslope-scale storm response. These isolated patches of subsurface saturation are located in topographic depressions in the impeding layer, and connection of these patches of (transient) saturation is controlled by both the topography and permeability of the impeding layer. The fill and spill theory was supported by observed patterns of transient water table development and lateral subsurface stormflow at Panola, and since

* Corresponding author. Address: The Pennsylvania State University, Department of Crop and Soil Sciences 116 Agricultural Sciences and Industry Building, University Park, PA 16802, USA. Tel.: +1 814 867 3074; fax: +1 814 863 7043.

E-mail address: cbg12@psu.edu (C.B. Graham).

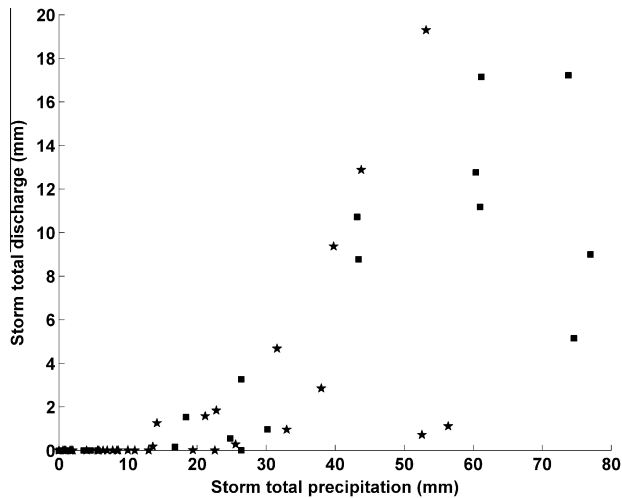


Fig. 1. Whole storm precipitation and hillslope discharge at instrumented Maimai hillslope. 150 days of monitoring included 125 storms (data from Woods and Rowe (1996) (stars) and Brammer (1996) (squares)).

then by model analysis in two and three dimensions (Hopp and McDonnell, 2009; Keim et al., 2006).

Despite the promise of fill and spill as a conceptual framework to explain whole-slope rainfall–runoff thresholds and emergent landscape behavior, physical measurement of the factors affecting fill and spill are rudimentary and poorly quantified at other sites. The mapping, measuring and quantifying the flow network activated during fill and spill and how these networks conspire with bedrock permeability has yet to be determined. Yet, this mapping and quantification is a critical research question in hillslope hydrology and essential for understanding whole-hillslope threshold processes and generalizing the fill and spill framework to other areas. However, such mapping and measurement is extremely difficult with current field techniques and approaches.

So how might we explore the mechanistic controls on hillslope threshold response to storm rainfall, explore further the fill and spill framework and develop a function that captures sub-grid scale variability into numerical macroscale behavior? Here we present a field-based experiment aimed at defining hillslope-scale internal controls on threshold response and whole hillslope emergent behavior via limited destructive sampling of a well-researched site. We follow in the tradition of soil science, where soil pits and excavations after tracer applications are a commonplace method for determining processes occurring at the soil pedon scale (Flury et al., 1995; Zehe and Flüher, 2001). Our work builds upon some destructive experimentation that has already been attempted in hillslope hydrology. Kitahara (1993) filled a network of macropores with plaster and removed the soil from surrounding the network, identifying the location and morphology of the preferential flow network. Additional pit scale irrigation and excavation experiments have been instrumental in revealing the structure and predominance of lateral and vertical preferential flow (Mosley, 1982; Noguchi et al., 2001; Weiler and Naef, 2003) but have been limited to the pedon scale and have not been attempted across a complete hillslope section. The only whole hillslope irrigation and excavation to date, by Anderson et al. (2009), has shown the power of such a destructive mapping approach and identified the subsurface flow network of a humid forested hillslope in British Columbia, Canada.

Here we show how destructive sampling at the hillslope scale can be especially useful at our well studied sites, where a history of observed field behaviors can be tested, *ex post facto*, using our forensic approach. Our research site is the Maimai Experimental Watershed on the South Island, New Zealand (see McGlynn et al. (2002) for review). Maimai was one of the early sites where lateral

subsurface stormflow was mechanistically assessed (Mosley, 1979, 1982). More recently, studies at Maimai have chronicled the initiation of subsurface stormflow through soil pipes (McDonnell, 1990), the patterns of subsurface stormflow (Woods and Rowe, 1996) and solute transport (Brammer, 1996) at the slope base, the relative role of hillslope vs. riparian zones in runoff initiation (McGlynn and McDonnell, 2003a) and nutrient and solute transport (McGlynn and McDonnell, 2003b). While the recognition of rainfall thresholds for generating hillslope response at Maimai date back to the original work of Mosley (1979), the controls on this whole-hillslope response have been difficult to assess, even at this intensively studied site.

At Maimai, many key components of the fill and spill theory have not yet been resolved. Both the nature of the lateral subsurface flow network and the permeability of the bedrock are poorly understood. The characteristics of the lateral flow network have been extrapolated from observations made at trench faces and limited, small scale excavations (<1 m²) (Weiler and McDonnell, 2007) while the upslope form, connectivity, extent of the lateral flow network remains unknown. While the bedrock permeability has been estimated using a catchment scale water balance (O'Loughlin et al., 1978; Pearce and Rowe, 1979), no direct measurements have been made. We posit that hillslope scale excavations are a powerful field method to reveal the existence and extent of the lateral flow network and a way to expose the bedrock surface for permeability measurements.

This paper details a hillslope scale irrigation – excavation experiment designed to identify the dominant flow pathways and the role of bedrock topography and permeability at the hillslope scale. Our work tests three sets of multiple working hypotheses directed at the first order controls on the fill and spill theory stemming from previous work at Maimai and other steep, forested hillslopes:

1. How can we characterize the lateral subsurface flow?
 - 1(a) Lateral subsurface storm flow is concentrated in the soil matrix and the preferential flow network is non-existent or unimportant in generating flow at the hillslope scale (supported at the site by Sklash et al. (1986)).
 - 1(b) A lateral preferential flow network exists, consisting of disconnected soil pipes located in the soil profile (supported at the site by McDonnell (1990), elsewhere by Noguchi et al. (2001)).
 - 1(c) A lateral preferential flow network exists, consisting of a connected network located at the soil/bedrock interface (supported at the site by Mosley (1979)).
2. How does the bedrock surface topography affect flow routing?
 - 2(a) The bedrock surface plays an indirect role in flow routing (supported at the site by Woods and Rowe (1997)).
 - 2(b) The bedrock surface determines flow routing (supported at the site by Freer et al. (1997) and McDonnell (1997), elsewhere by Freer et al. (2002)).
3. How does the permeability of the lower boundary affect flow processes?
 - 3(a) The bedrock is effectively impermeable (supported at the site by McDonnell (1990), Mosley (1979), O'Loughlin et al. (1978), and Woods and Rowe (1996)).
 - 3(b) The bedrock permeability is high enough to have a significant impact on flow processes (supported elsewhere by Onda et al. (2001), Tromp-van Meerveld et al. (2006) and Hopp and McDonnell (2009)).

Site description

The experiments were performed at the Maimai Experimental Watershed, near Reefton, South Island, New Zealand (Fig. 2).

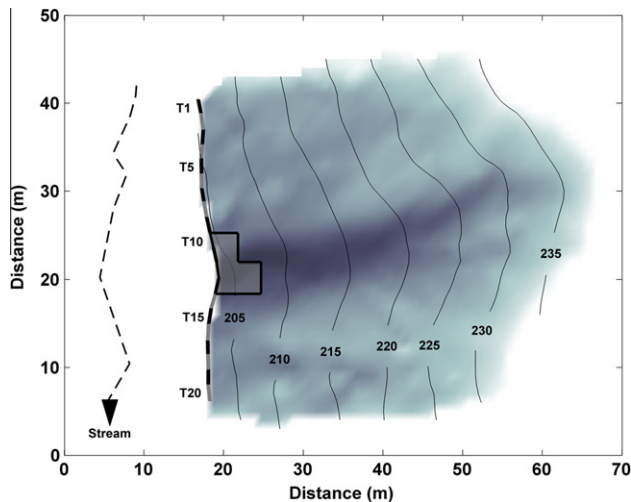


Fig. 2. Maimai instrumented hillslope with excavation locations (grey box). Selected trench sections (T1–T20) are labeled.

Maimai was established as a hydrological experimental field site in late 1974, to examine the effects of forest management on water and sediment flux. The site has been continuously monitored since.

Soils are stony silt loam podzolized yellow brown earths (Rowe et al., 1994) overlain with a 15 cm thick high porosity organic humus layer (McDonnell et al., 1991). Hydraulic conductivity of the mineral soils range from 5 to 300 mm/h, the mean porosity is 45%, and soil profiles average 60 cm (McDonnell, 1990). The soil has a high density of preferential flow paths, including vertical cracks, live and dead root channels, and macropores in the soil profile and along the soil bedrock interface (Brammer, 1996; Mosley, 1979; Woods and Rowe, 1996). At the soil surface lies a high permeability (hydraulic conductivity >1000 mm/h (McDonnell et al., 1991)) organic mat, where isolated and short lived downslope preferential flow has been observed. Due to the high annual rainfall (2450 mm mean annual rainfall (Woods and Rowe, 1996)) and high storm frequency (average time between storms ~3 days), soils remain within 10% of saturation through most of the hydrologic year (Mosley, 1979). Considered poorly permeable with annual leakage estimated at 100 mm/year (Pearce and Rowe, 1979), the bedrock is Early Pleistocene Conglomerate of the Old Man Gravel formation, a moderately weathered, firmly compacted conglomerate with clasts of sandstone, schist and granite in a clay-sand matrix (Rowe et al., 1994).

Catchments are highly responsive, with a runoff ratio (catchment discharge/rainfall) of 54% annually, of which 65% is quickflow (Pearce et al., 1986), as defined by Hewlett and Hibbert (1967). The hillslopes have a much lower runoff ratio, ~15%, and baseflow greater than 0.25 L/h (1.17E–4 mm/h) for more than 4 days after an event has not been observed (Woods and Rowe, 1996). Reviews by McGlynn et al. (2002) and Rowe et al. (1994) provide additional details on the Maimai catchments.

Our experiments were performed at the hillslope instrumented by Woods and Rowe (1996). The relatively planar hillslope was chosen for their studies, downstream of the M8 catchment studied by earlier generations of scientists (McDonnell, 1990; Mosley, 1979, 1982; Pearce et al., 1986; Sklash et al., 1986). The hillslope is representative of the Maimai slope lengths and gradients, with a maximum slope length of 50 m, and gradients above 35°. Lateral subsurface flow is collected at the slope base by a 60 m long trench excavated into the conglomerate bedrock surface. Flow from the hillslope is routed to thirty 1.7 m trench sections and then into recording one liter tipping buckets. Due to soil instability and a

deep profile, the trench is split into two groups of 20 and 10 trench sections, with a 10 m gap in between. Woods and Rowe (1996) monitored subsurface flow at the trench for 110 days in 1993. A key finding from their work was the recognition of the large spatial variability of lateral subsurface flow, something subsequently observed at field sites around the world (Freer et al., 2002; Hutchinson and Moore, 2000; Kim et al., 2004). While Woods and Rowe (1996) attributed the spatial variability of lateral subsurface flow to surface topography, subsequent analysis suggested that subsurface topography of the soil–bedrock interface might better explain the coarse patterns of flow distribution at the hillslope scale (Freer et al., 1997). Later work by Brammer (1996) monitored flow from the trench for 65 days and traced the flux of an applied line source bromide tracer at the instrumented hillslope 35 m upslope of the trench face and observed very fast subsurface stormflow tracer velocities, with 4% of tracer recovery in the first storm after application, less than 3 days later, and less than 9 h after the storm began.

Analysis of data records from the Woods and Rowe (1996) and Brammer (1996) storm monitoring demonstrate a clear threshold for lateral subsurface flow at the monitored hillslope at Maimai. If one defines an individual storm as at least 1 mm rain preceded by 24 h without 1 mm rain, 41 storms are identified in the Woods and Rowe dataset, with between 1 and 83 mm total precipitation (Fig. 1). Total storm hillslope discharge was defined as the increase in discharge for the duration of the storm, including 24 h after rainfall ceased. Total storm discharge ranged from 0 to 22.2 mm. For all events with less than 23 mm total storm precipitation, only one storm had measured discharge greater than 0 mm (0.19 mm discharge for a storm of 16.8 mm precipitation).

We reactivated sections 10–13 of the Woods and Rowe (1996) trench. These trench sections are located in a (surface and bedrock) topographic hollow where the majority of flow (>64%) was observed in both the Woods and Rowe (1996) and Brammer (1996) monitoring. Trench sections 10–13 drain upslope contributing areas between 51 and 473 m², and peak flows ranged from

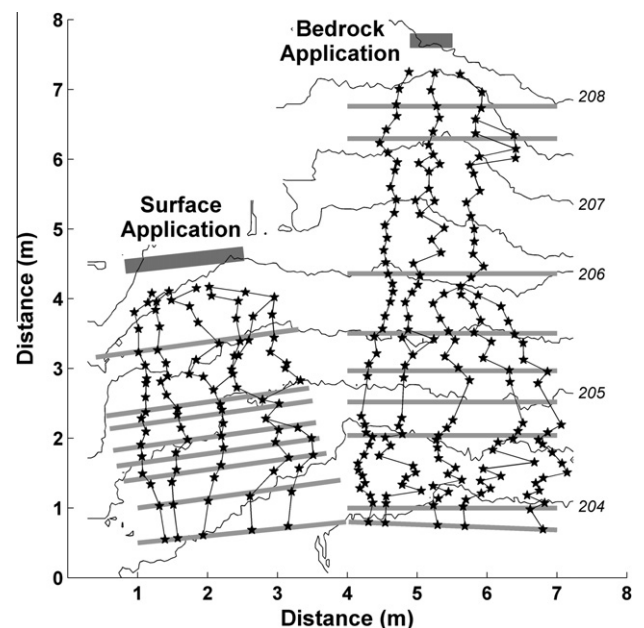


Fig. 3. Bedrock topography of excavated area and application sites with 0.5 m contour intervals above an arbitrary datum. (a) Locations of exposed soil face during bromide tracer injections (grey) for surface and direct soil bedrock interface applications. (b) Preferential flow observations for an additional 2–3 slices between each tracer injection (stars indicate locations of observed preferential flow).

0.17 to 0.23 L/s (0.23–2.01 mm/h) during storm monitoring. In this area of hillslope, pipe flow at the trench face was observed by previous researchers to dominate lateral subsurface flow (Woods and Rowe, 1996). Overland flow has not been observed at the hillslope.

Methods

We performed two sets of irrigation experiments above trench sections 10–13 (Fig. 3). The first experiment was a subsurface injection of water and tracer 8 m upslope of trench sections 12–13. The second experiment was a water and tracer line source surface application 4 m upslope of the trench sections 10–11. The upslope application distance was constrained by the presence of a 25 year old *Radiata Pine* 5 m upslope of the trench face. Water was pumped 20 m from the first order stream draining the M8 catchment to the application site with a small gas pump. Irrigation continued until steady state conditions were reached, as determined by steady discharge measured at the trench, and constant spatial patterns of flow at the trench face. For the deep injection experiment, the water was pumped directly into a soil pit excavated to the soil bedrock interface 8 m upslope of the trench face. The pit was 0.6 m deep, roughly cylindrical with a radius of 0.3 m. For the surface application, water was pumped to a perforated trough 1.7 m long. Water irrigated the soil surface evenly along the 1.7 m long by 0.1 m wide trough, and the perforations were spaced 25 mm apart so that a constant shallow (<25 mm) water level was maintained in the trough. Due to fluctuations in the water source (related to creek stage and pumping rate), the application rate was not constant during the 4 weeks of experimentation. However, steady application was possible over 2–3 h application periods through careful monitoring of stream levels. Application rate was measured on site, and varied between 0.02 L/s and 0.30 L/s. Discharge was measured at the trench face using the Woods and Rowe (1996) guttering and tipping buckets, linked to a CR10 Campbell Scientific datalogger. As the excavations continued, much of the trench section was damaged, so subsequent trench discharge rates were not recorded. All hillslope discharge was routed to a common 5 L collection vessel where tracer concentration was measured.

Excavation and flow mapping

After steady state was reached in each of the experiments, the types and locations of dominant flow pathways were recorded at the trench face. To assist photographic recording of flowpaths, brilliant blue dye (CI Food Blue #2; CI 42090; $C_{37}H_{34}N_2Na_2O_9S_3$) was added to the irrigation water. At steady state, the dominant flow-path discharge points on the exposed soil face were labeled with orange tape, and vertical and lateral coordinates were recorded. Both matrix flow (as evidenced by wetness at the seepage face) and macropore or other preferential flowpaths were identified. A digital photograph was taken of each exposed trench slice, and of each noted flowpath for later analysis. After the flowpath types and locations were identified and recorded, 0.2–0.4 m thick, 3–4 m wide slices of the full soil profile were removed upslope from the trench face. As the soil was removed, the major flowpaths were traced upslope towards the application location to develop a near continuous map of lateral flow throughout the hillslope length. The bedrock surface was fully exposed after each slice removal and the new flow locations and flow features along the soil bedrock boundary were identified. For the pit experiment, 8.0 m of soil was removed upslope in 37 slices. For the surface application, 4.0 m of soil was removed in 18 slices. In both case, irrigation was effectively continuous throughout the excavation process.

Tracer injections

We measured tracer velocities between excavations by adding a Br^- solution to irrigation water. Tracer was added at every second or third steady state water application following soil removal (nine times during the pit application experiment (when 0, 1.30, 1.90, 2.45, 2.84, 3.13, 4.19, 6.62 and 7.60 m soil had been removed) and seven times during the surface application experiment (when 0.50, 0.98, 1.25, 1.53, 1.92, 2.15, and 3.20 m soil removed)) (Fig. 3). During the surface application experiment, four additional tracer injections were added at different irrigation rates with 125 cm soil removed. An ion selective electrode for Br^- (TempHion®, Instrumentation Northwest, Inc.) was placed in a 5 L tank at the trench and readings were taken every minute. 15 g Br^- was injected directly into the excavated pit during Experiment 1 and uniformly along the length of the gutter during Experiment 2. The water application rate was held constant during the injection, and continued until Br^- concentration returned to within 200% of the background concentration, or as long as conditions would allow. Flow rates during the Br^- injection ranged from 0.03 to 0.11 L/s. Due to low flow conditions, irrigation water was recycled in some experiments, causing Br^- concentration to remain higher than background. In these cases, water application and tracer monitoring continued until steady concentration at the trench face was reached. While a mass recovery was not possible, due to deterioration of the trench face, a representative sample of the discharge was collected for all injections.

Bedrock permeability

The bedrock hydraulic conductivity was measured using a falling head test. A cylindrical pit was excavated into the Old Man Gravel bedrock 2 m upslope of the trench, 10 m downstream of the area used for the irrigation experiments. The pit was 25 cm deep with radius 17 cm, with a cross sectional surface area of 934 cm² and total surface area including the pit walls and bottom of 2777 cm². The bedrock was relatively soft and no fracturing was observed as the pit was excavated. A 1 mm resolution recording capacitance water level recorder (TruTrack, Inc., model WT-HR) was placed in the pit to record water height changes over time. Prior to the experiment, the pit was prewetted by maintaining a constant head of water for 5 h. The pit was then filled with 9 L of water, to a depth of 17 cm. The water in the pit was allowed to drain for 13 h. Initial and final water levels were measured with a ruler to confirm capacitance rod function. The recession of the water table was fit to a quadratic power law. The hydraulic conductivity was calculated using Darcy's law assuming a unit head



Fig. 4. Exposed bedrock surface with locations of surface and soil bedrock interface water and tracer applications.

gradient at long time, and infiltration along either the pit bottom or the pit bottom and sides.

Results

Flow routing and locations

Over the course of the irrigation/excavation experiment, 24 m² soil was removed (Fig. 4), while subsurface flow paths were tracked 4–8 m upslope of the original exposed soil face. During both irrigation experiments, lateral subsurface flow at the hillslope trench was dominated by concentrated flow at the soil bedrock interface, including both sheet flow (thin (<2 mm), low volume diffuse flow spread over 5–20 cm width) and concentrated flow in distinct pipes (high volume flow in visible gaps at the base of the soil profile). The bedrock surface was characterized by medium sized cobbles (cobble diameter ~2–5 cm) embedded in a schist matrix. These cobbles and the schist matrix between them resulted in small topographic pools in the bedrock surface, generally less than 1 cm deep and 5 cm in diameter. During the first water application of Experiment 2 (surface application), flow at the trench was restricted to within 5 cm of the soil bedrock interface. At the trench face, flow was concentrated in five pipes connected by sheet flow along the bedrock surface. An estimated 70% of total lateral subsurface flow was in the concentrated flowpaths, with the remainder in sheet flow. The concentrated areas were generally voids between the bedrock surface and lower soil boundary, rather than decayed root channels or worm tunnels. These voids were less than 5–10 mm high and ranged from 10 to 100 mm wide and often filled with live tree roots (see Fig. 5 for an example exposed trench face 50 cm upslope of the trench).

After flow locations were recorded, 20 cm soil was removed from the trench face, with the areas of concentrated flow traced upslope as the soil was excavated. This process was then repeated as the hillslope was excavated. As excavation progressed upslope in 20–40 cm increments, the flowpaths remained continuous and connected, with some divergence and convergence, controlled by bedrock features such as cobbles, microscale valleys and ridges in the bedrock surface. A coat of brown organic staining was observed on the exposed bedrock surface, along with a nearly ubiquitous mat of very fine to medium live roots along the bedrock surface (Fig. 6). In some isolated locations water diverged from the bedrock surface and flowed through and above a thin (<100 mm) gleyed clay layer. These gleyed areas of soil appeared to be in topographic depressions in the bedrock surface, and suggest chronically saturated conditions.

Vertical preferential flowpaths were observed in the exposed vertical soil column in the immediate proximity of where the water and dye were applied. Such features were not active in the slices greater than 0.75 m downslope from the surface application. With the exception of limited matrix flow and some isolated macropores, the majority of water traveling from the soil surface to the bedrock was via thin, sub-vertical cracks in the soil, similar to those reported by previous researchers (McDonnell, 1990). These cracks were coated with a brown organic stain, similar to that seen on the bedrock surface. The vertical and sub-vertical cracks were planes of weakness in the soil structure, and slaked off while excavating.

For the deep injection experiment, flow was observed at the soil bedrock interface at all excavated slices, as well as during excavations between slices. Once excavations reached within 30 cm of the pit, some flow through the soil column was observed in the lower



Fig. 5. Exposed evidence for preferential flow at the soil bedrock interface. (a) Preferential flow during experiment at soil bedrock interface with live roots. (b) Organic staining on bedrock surface indicating persistent flow at the soil bedrock interface.

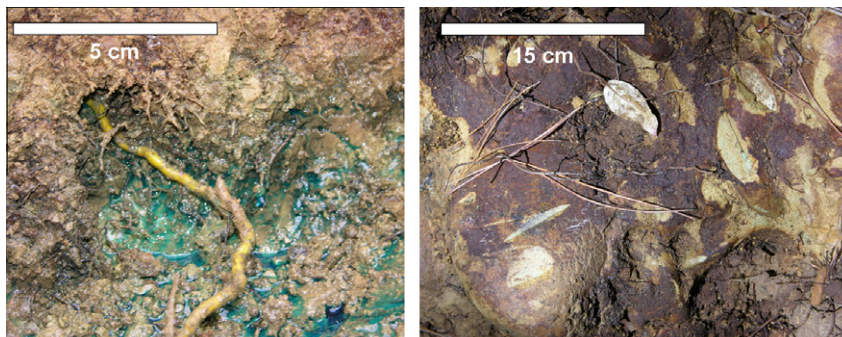


Fig. 6. Exposed soil face after 0.5 m soil removed, 3.5 m downslope of surface application of dye and water. Note 4–5 areas of concentrated flow, coinciding with brown organic staining in lower soil profile.

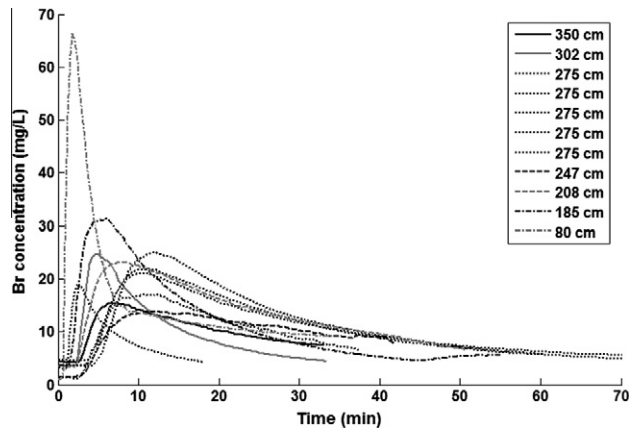


Fig. 7. Tracer breakthrough at trench face of Br-tracer applied on soil surface. Tracer was applied 4 m upslope of the trench, with 0.8–3.5 m soil remaining between tracer application and exposed soil face.

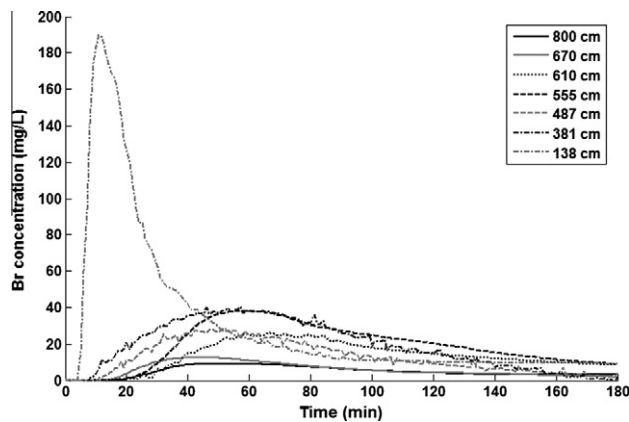


Fig. 8. Tracer breakthrough at trench face of Br-tracer applied directly to soil bedrock interface. Tracer was applied 8 m upslope of the trench, with 3.8–8.0 m soil remaining between tracer application and exposed soil face.

25 cm of soil. At this point both active macropore flow in the soil profile and saturated matrix flow were observed. The macropores were less than 10 cm long, and appeared disconnected from any larger preferential flow system.

Trench response more than 75 cm downslope of the surface application and 30 cm downslope of the pit application was identical for the two application regimes in terms of flowpath location (at the soil bedrock interface), morphology (areas of concentration controlled by bedrock depressions and obstructions connected by

sheet flow), and flow response (rapid and sensitive to changes in application rate). Fluctuations in application rate, which varied from 0.07 to 0.25 L/s, did not have an impact on the locations of concentrated flow, though the relative magnitude of each flow path was sensitive to input rate.

Field observation and visual analysis of photographs of each trench section showed areas of organic staining in the lower profile (see Fig. 6). This staining suggested areas of prolonged saturated conditions, and concentrated above the flow paths identified during the irrigation experiments. Stained areas were generally semi-circular, with a diameter of up to 10 cm, and located with the base on the bedrock surface. Additional staining was observed along the entire bedrock surface, while little was seen in the soil profile greater than 10 cm above the bedrock surface.

Tracer breakthrough and velocity

Tracer breakthrough was similar for both the surface and direct bedrock injections, with initial tracer breakthrough averaging seven (17 for direct bedrock injection) minutes after application (Figs. 7 and 8, Tables 1 and 2). Peak concentrations were reached in 18 (45 for direct bedrock) minutes. The time to initial and peak concentration breakthrough were longer for the direct bedrock injection than the surface injection, as expected due to the longer travel distance (8 m as opposed to 4 m). Breakthrough curves were skewed to the right, with a rapid peak and long tail. A skewed breakthrough curve indicates transport with a range of travel velocities, consistent with the combination of bedrock sheet flow and concentrated flow observed during excavation. Due to irrigation source water limitations, time constraints and pumping difficulties, the entire tail was not captured for the tracer experiments. Deterioration of the trench flow collecting system precluded an accurate mass balance for the tracer injections using the water and tracer output. Using the input flow rate, and assuming that leakage into the bedrock was not significant during the time span of the tracer experiments (<3 h), mass recovery rates were calculated (Figs. 9 and 10), ranging from 11% to 61% for the surface application, and 34–75% for the direct bedrock application (Tables 1 and 2).

Despite these difficulties, the time to initial rise and time to peak tracer concentrations were well captured, giving an estimate of initial and peak travel velocities. For the surface applications, initial breakthrough velocities ranged from $6.7E-3$ to $3.3E-2$ m/s (Table 2). For Br^- injections with greater than 1 m soil remaining downslope of the irrigation source, initial breakthrough velocity was uncorrelated with the amount of soil removed ($R^2 = 0.12$). Peak concentration velocities ranged from $2.1E-3$ to $1.3E-2$ m/s, with no correlation between tracer velocity and soil removal

Table 1
Tracer breakthrough data for surface application. Active pore volume is computed as volume of water discharged before peak concentration reached. Multiple tracer applications were performed at 2.75 m, with different input flow rates. The mass recovery of the tracer was affected by the variable amount of irrigation after the peak concentration was observed.

Distance to exposed soil face (m)	Total pore volume (m^3)	Input rate (ml/s)	Time to initial rise (min)	Time to peak (min)	Peak velocity (m/s)	Mass recovery (%)	Active pore volume (m^3)	Active pore volume (%)
3.5	2.69	95	8	20	$2.92E-03$	22	0.11	4.08
3.02	2.32	90	8	18	$3.24E-03$	25	0.10	4.30
2.75	2.12	45	7	32	$1.82E-03$	11	0.09	4.25
2.75	2.12	90	10	18	$3.24E-03$	40	0.10	4.73
2.75	2.12	170	7	14	$4.17E-03$	47	0.14	6.62
2.75	2.12	226	5	11	$5.30E-03$	55	0.15	7.09
2.75	2.12	305	4	10	$5.83E-03$	61	0.18	8.51
2.47	1.90	109	8	28	$2.08E-03$	41	0.18	9.47
2.08	1.60	96	7	22	$2.65E-03$	56	0.13	8.12
1.85	1.42	81	5	19	$3.07E-03$	49	0.09	6.32
0.8	0.62	123	2	5	$1.17E-02$	53	0.04	6.50

Table 2
Tracer breakthrough data for direct bedrock application.

Distance to exposed soil face (m)	Total pore volume (m ³)	Input rate (ml/s)	Time to initial rise (min)	Time to peak (min)	Peak velocity (m/s)	Mass recovery (%)	Active pore volume (m ³)	Active pore volume (%)
8.00	4.97	97	20	53	2.52E-03	34	0.31	6.24
6.70	4.16	105	17	42	3.17E-03	39	0.26	6.25
6.10	3.79	63	30	66	2.02E-03	61	0.25	6.60
5.55	3.45	58	25	54	2.47E-03	83	0.19	5.51
4.87	3.02	56	22	47	2.84E-03	47	0.16	5.29
3.81	2.37	43	11	52	2.56E-03	59	0.13	5.49
1.38	0.86	60	6	14	9.52E-03	95	0.05	5.83

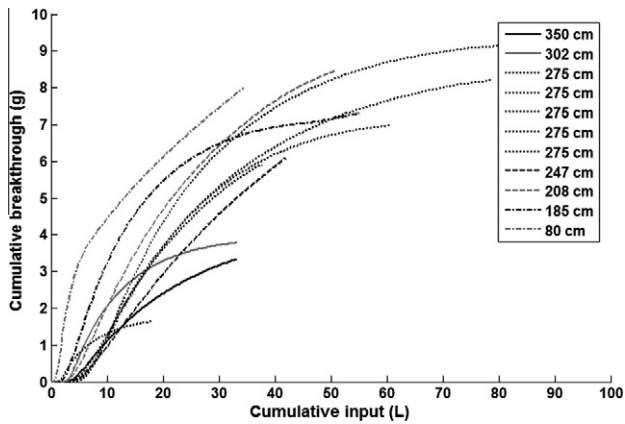


Fig. 9. Cumulative tracer breakthrough from surface applications, with 0.8–3.5 m soil remaining between tracer application and exposed soil face. 15 g of tracer was added for each application.

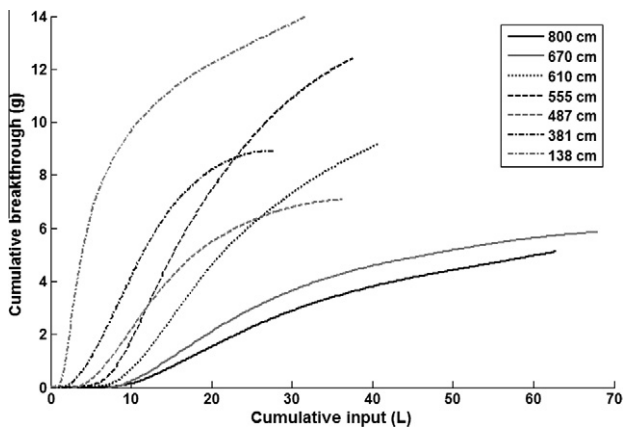


Fig. 10. Cumulative tracer breakthrough from direct bedrock applications, with 3.8–8.0 m soil remaining between tracer application and exposed soil face. 15 g of tracer was added for each application.

($R^2 = 0.02$). For the pit application, initial and peak velocities ranged from $5.3E-3$ to $6.7E-2$ m/s and $1.9E-3$ to $3.3E-2$ m/s, respectively. For the pit application, initial breakthrough and peak concentration velocities were not correlated with soil removal ($R^2 = 0.05$ and 0.0 respectively), where velocity increased as the soil mass was removed (Tables 1 and 2).

For the initial applications, while the trench system was still intact, we calculated the volume of water discharged from the trench before the peak concentration was reached, based on measurement of input rates and trench runoff. This represented the volume of water in the active flow paths, or the active pore volume. The active pore volumes in these experiments ranged from 0.04 m³ to 0.18 m³ for the surface application, and 0.03 to 0.31 m³ for the direct bedrock application. The active pore volumes averaged 6% of

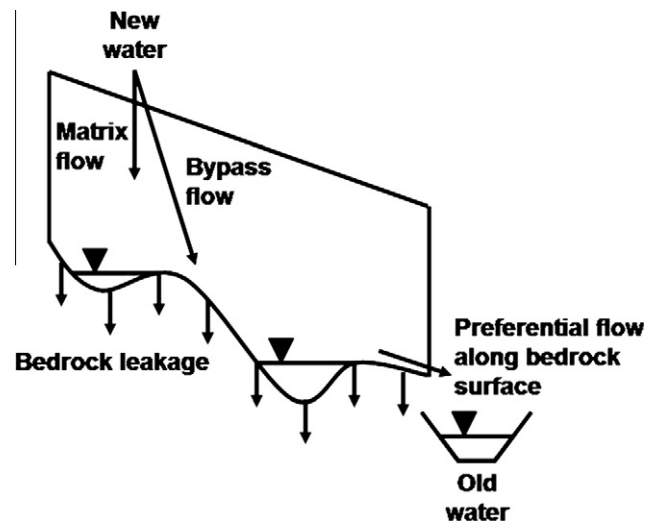


Fig. 11. New perceptual model of lateral subsurface flow at the Maimai hillslope.

the total estimated pore volume for both the surface and direct bedrock applications, based on an average soil depth of 0.6 m and porosity of 0.45 reported at the site (McGlynn et al., 2002). Additionally the initial breakthrough time of the tracer was also recorded (Table 1). The corresponding input volume before initial breakthrough ranged from 0.6 to 3.0 L.

Peak concentration velocities were high, ranging from $1.9E-3$ to $6.7E-2$ m/s and 6.8 to 120 m/h for the two sets of injections. With the entire soil profile intact, the tracer velocity was $3.3E-3$ m/s for the surface and $2.5E-3$ m/s for the direct bedrock injection (Table 1). Our reported peak concentration velocities likely overestimate mean travel velocities. Assuming Darcy regime flow, a measured soil saturated hydraulic conductivity (k_{sat}) of 0.01–0.30 m/h (McDonnell, 1990), the measured average hillslope gradient (s) of 56%, and porosity (f) of 0.45, Darcy ($v = k_{sat}s/f$) velocities would be predicted in the range $3.8E-6$ – $1.04E-4$ m/s (0.013 – 0.373 m/h), more than two orders of magnitude less than that measured in our experiments.

Bedrock permeability

The drainage rate of pooled water in the bedrock permeability experiment decreased during the first 9 h, with an initial rate of $1.8E-6$ m/s (0.64 cm/h), slowing to a steady rate of $8.6E-7$ m/s (0.31 cm/h) for the final 4 h of the experiment. Assuming a unit head gradient at long time, the bedrock hydraulic conductivity was calculated from Darcy's Law ($Q = K_s A (\Delta h/L)$), where Q is pit drainage at late time, K_s is the hydraulic conductivity, A is the area over which drainage occurs, $\Delta h/L$ is the head gradient, assumed to near 1 at long time. Two estimates of A were made: (1) if drainage occurred only at the base of the pit, $A = 935$ cm² and (2) if drainage occurs over the entire surface area of the pit, $A = 935 + 1842$ cm².

Using assumption (1), the bedrock hydraulic conductivity was $8.6E-7$ m/s (0.31 cm/h). Using assumption (2) the hydraulic conductivity was $2.9E-7$ m/s (0.10 cm/h). The recession of the water table was also well fit ($R^2 = 0.995$) by a function of the form $z_t = z_{t-1}(1 - \Delta t/\tau)$, where τ is the characteristic time scale for the water table recession. Using a least squares optimization, $\tau = 11.9$ h ($4.28E4$ s) ($R^2 = 0.995$).

Discussion

Our experiments represent the first hillslope scale destructive sample sampling at Maimai or any other hillslope with an extensive scientific history that we are aware of. This targeted destructive sampling was designed to explore fill and spill as a conceptual framework and to isolate and illuminate the preferential flow network long hypothesized to dominate lateral subsurface flow at the site. This excavation allowed for the additional measurement of the permeability of the bedrock, a crucial control on the initiation of lateral subsurface flow and the partitioning of the water balance. The work was specifically designed to test three sets of competing alternative hypotheses related to the nature of the lateral subsurface flow and its relationship with the topography and permeability of the bedrock. The first set of hypotheses addresses the form and function of the preferential flow network; the second set of hypotheses addresses the role of the bedrock topography on the flow network; the third set of hypotheses addresses the permeability of the bedrock. The three sets of hypotheses are investigated in depth below. We then discuss the influence of our findings on the threshold relation between storm total precipitation and lateral hillslope discharge. A new perceptual model of flow at the site is developed, and its implications regarding model structure are discussed in detail in an accompanying manuscript (Graham and McDonnell, this issue).

Preferential flow network

We rejected hypotheses 1a and 1b, and accepted hypothesis 1c – that lateral subsurface flow is dominated by a connected preferential flow network located at the soil bedrock interface. Applied flow rates were consistent with lateral flow observed during medium to large stormflow, and the preferential flow network was able to accommodate the flow volumes. Lateral subsurface flow was observed solely at the soil bedrock interface, where water was transmitted both as sheet flow and preferentially in voids restricted to within 5 cm above the bedrock surface, occupying only 4% of the available pore space. The active flow zone coincided with live and dead roots at the soil–bedrock interface and organic staining on the bedrock surface and in the lower soil profile, indicating these flow paths are stationary and chronically saturated during natural events. Both the root density and organic staining were much reduced in the soil profile above the observed flow zone. There was no evidence for lateral macropore flow within the soil profile as hypothesized by Weiler and McDonnell (2007) and observed elsewhere (Tsuboyama et al., 1994), though vertical and sub-vertical cracks appeared responsible for routing water from the soil surface to depth, as observed at this site (McDonnell, 1990). While some macropores were seen within the soil profile, these were apparently disconnected from the flow occurring at depth, and not observed to be routing water except near the irrigation application source.

While our irrigation rates were high when expressed as a precipitation rate (592–2117 mm/h, assuming an area equal to the surface area of the application gutter (0.17 m²)), our intent was to isolate the lateral subsurface flow component, rather than identify flow paths from the soil surface to depth. Measured lateral sub-

surface flow rates for natural storms at the gauged trench face for trench sections 12–13 (below the pit application) range from 0 to 0.40 L/s (Woods and Rowe, 1996), which bound our applied rates and measured discharge. Downslope of the surface application, measured throughflow for trench sections 10–11 during natural events were similar (0–0.38 L/s). Considering the relatively small contributing area between the application site and the collection trench, most of the water collected at the trench would pass the application site as lateral subsurface flow during natural events. The effect of a trench face on unsaturated flow paths has long been known (Atkinson, 1978), primarily diverging flow vectors from the trench face due to capillarity and other edge effects. Since our system was dominated by saturated flow, edge effects were not anticipated to be a large factor. In fact, no evidence of edge effects due to the trench face was seen while excavating upslope during the irrigation and no evidence of unsaturated matrix flow (staining of the dyed irrigation water in the soil profile) was seen upslope of the original trench.

Mosley (1979) identified bypass flow to the bedrock surface and downslope routing along the bedrock as one of the major lateral subsurface flow paths from pit excavations in the M8 catchment. During small scale irrigation experiments (application <1 m upslope from his 1 m² pits), Mosley measured very fast flow velocities (average 6 m/h) along these and other flowpaths. These findings were seemingly contradicted by the age of the water (~4 months) and low percentage (<25%) of event water in pit discharge, as identified by analysis of naturally occurring oxygen and hydrogen isotopes in the rainfall (Pearce et al., 1986; Sklash et al., 1986). One possible source of mixing of event and stored, pre-event water is in the soil profile, as rainfall mixes in the large soil moisture reservoir before leaking onto the bedrock surface and rapidly routing downslope. This is consistent with the observed lack of downslope aging of water at M8 at the hillslope scale (Stewart and McDonnell, 1991).

This network differs from previous conceptual models in that it is connected, extensive, and located exclusively at the soil bedrock interface. Tani (1997) proposed a similar network after stormflow monitoring at Minamitani catchments, Japan, though bedrock interfacial flow was perceived to begin there after soil profile saturation. In an irrigation/excavation experiment at Hitachi Ohta, Japan, where irrigation was applied evenly on the surface 1 m upslope of a trench, Tsuboyama et al. (1994) showed that flow was dominated by matrix flow and laterally oriented pipes connected by organic rich areas of mesoporosity, while flow along the bedrock interface played a relatively minor role. The findings of the current experiment suggest that a very different flow network may have been observed at Hitachi Ohta had the irrigation been applied further upslope, allowing the irrigated water the time to reach the bedrock surface. At Panola Georgia, storm monitoring by Tromp-van Meerveld and McDonnell (2006a) showed that flow from macropores located at the soil bedrock interface makes up 42% annually of trenchflow at a site where leakage to the bedrock dominates the water balance. The lack of upslope excavations or similar investigations has prevented the determination of the upslope nature of the flowpath network at Panola, though this research suggests that a connected preferential flow network at the soil bedrock interface is possible.

Bedrock surface flow routing

We rejected hypothesis 2a and accepted hypothesis 2b – that the bedrock surface controls lateral subsurface stormflow routing. The bedrock micro and macrotopography were shown to be the major control of water routing at the hillslope scale. While occasionally the flow paths in the soil were observed above the soil bedrock interface on top of thin clay lenses, the majority of flow

was in direct contact with the bedrock surface. During the excavations interfacial flow paths were observed to be routed primarily by features such as protruding cobbles and rills on the bedrock surface. Due to the steep slopes and generally planar bedrock, much of the flow routing was controlled by microtopographic features that were small, less than 10 cm in relief. In one case, flow was observed to be routed from one collecting trench section to another by one such small rill on the bedrock surface 1 m upslope of the trench. This feature had a maximum relief of 5 cm and routed approximately one third of the water from one trench section to the next, locally redirecting water fed by 500 m² of upslope contributing area to the site. Since water reached the bedrock surface within one meter of application for both the pit and surface application, bedrock routing would be expected to dominate flow paths for the majority of water upslope of the collecting trench.

Freer et al. (1997) used a two meter DEM of the bedrock topography to determine hillslope scale flow routing at the Maimai hillslope and observed that it was a better predictor of the spatial pattern of hillslope trench flow than surface topography. Woods and Rowe (1997), however, showed that the difference was slight, and could be explained by uncertainty in the surface topography, where small errors in the DEM could result in large differences in the upslope contributing area at each two meter trench section. The findings from the present study suggest that small topographic features can have a disproportionately large impact on flow routing at the two meter scale. Furthermore, the 2 m DEM of bedrock topography used by Freer et al. (1997) was not likely of high enough resolution to reliably predict flow at the two meter trench section scale. From the present study, it seems that a very high resolution DEM (<10 cm in each direction) of the bedrock surface is needed to predict flow as measured by two meter trench sections located at the hillslope base. While both the surface and subsurface two meter DEMs predicted the general pattern of flow (concentrated in the topographic hollow), neither is of sufficient precision to predict flow into each trench section.

Bedrock permeability

We rejected hypothesis 3a and accepted hypothesis 3b – that the bedrock permeability is significant in this hillslope. The measured bedrock hydraulic conductivity is classified as semipervious (Bear, 1972) and could result in leakage into the bedrock becoming a potentially a large component of the water balance. The bedrock at Maimai has been described as “poorly permeable” (O’Loughlin et al., 1978), “effectively impermeable” (McDonnell, 1990), and as “nearly impermeable” (McGlynn et al., 2002). However, to our knowledge, no direct measurements of bedrock permeability have ever been attempted at Maimai. Our falling head permeability measurement showed that bedrock K_{sat} was far from impermeable (2.9E–7–8.6E–7 m/s (0.1–0.3 cm/h)). While this was one point measurement of limited scale, the relatively high value suggests that losses to bedrock cannot be ignored.

There is evidence in the historic data record of significant losses to bedrock at the Maimai hillslope. At the nearby M8 catchment (a 3.8 ha zero order catchment whose outlet is 100 m upstream of the study hillslope in this paper) annual runoff ratios measured at a perennial stream average 54% (1404 mm) (McGlynn et al., 2002). Barring any lateral redistribution from nearby catchments and assuming no losses to deep groundwater, this suggests a maximum annual evaporation rate of 46% of precipitation (1196 mm). The hillslope-scale runoff ratios have been reported to be 13% for the 110 day experiment (Woods and Rowe, 1996), and 14% for the 90 day experiment (Brammer, 1996). While not encompassing annual variations, the lack of seasonality at the site suggests that changes in storage at the hillslope would be minor. Since both sites are experiencing similar evaporative conditions, the difference in

runoff ratios is likely due to leakage to the bedrock, which is likely to be a sink at the hillslope scale, and a source for stream channels. This would suggest a minimum loss to bedrock at the hillslope scale of 41% of rainfall (1066 mm/year (3.4E–8 m/s)). Previous estimates at the M8 catchment place bedrock leakage at 100 mm/year (O’Loughlin et al., 1978), or 3.9% of precipitation. The hillslope scale estimates are an order of magnitude larger than previous estimates. We hypothesize that the majority of this “lost” water would reemerge at the stream channel, based on the higher annual runoff ratios measured at the stream channel. This hypothesis is supported by the increase in runoff ratios observed by McGlynn et al. (2003a) at the event scale when moving from the hillslope to catchment scale. While not having an impact on the catchment water balance, water traveling through the bedrock and reemerging at the stream would have longer flow paths, more contact with the subsurface, different chemical composition and longer mean residence times.

This finding of the relatively high permeability at a site where the bedrock has been previously considered “effectively impermeable” (McDonnell, 1990) suggests that a similar reassessment is warranted at other hillslopes. In fact, leakage to bedrock has been shown to be a significant subsurface flowpath at the hillslope scale at a number of research catchments that were considered impermeable prior to investigation, with a wide range of underlying bedrock types (Hornberger et al., 1991; Katsuyama et al., 2005; Montgomery et al., 1997; Onda et al., 2001; Tromp-van Meerveld et al., 2006). Low runoff ratios observed at the monitored hillslope in Panola, Georgia (underlain by Panola Granite) were initially attributed to transpiration losses, before direct measurement of the bedrock permeability estimated it at 0.5 cm/h (Tromp-van Meerveld et al., 2006), approximately double that measured at Maimai in this study. Waichler et al. (2005) showed through numeric modeling that bedrock leakage accounts for 15% of the water balance at 3 second and third order catchments in the HJ Andrews Experimental Forest in Oregon (underlain by Andesite), a volume that was previously assumed to be lost to evaporation. Subsurface flow through the bedrock has been shown to be significant in other steep, forested catchments (e.g. Onda et al., 2001 (Serpentine Rocks); Montgomery et al., 1997 (Eocene Sandstone); Katsuyama et al., 2005 (weathered granite)), affecting mean residence times, tracer transport, and flow routing.

A new perceptual model of subsurface flow at Maimai

Based on the experimental results described above, the perceptual model of subsurface flow processes proposed by previous research at Maimai (summarized by McGlynn et al. (2002)) is modified to fit our new findings of subsurface flow processes at the site (Fig. 11). Perceptual models at Maimai have evolved over the years but have all been somewhat limited by isolated observations of water balance components (Mosley, 1979; Pearce et al., 1986), the spatial limitation of previous sprinkler experiments (McDonnell et al., 1991; Mosley, 1979), and the limiting nature of measurement techniques (Brammer, 1996; Woods and Rowe, 1996).

Our new perceptual model of flow processes at the Maimai hillslopes is consistent with previous findings in terms of how water moves to depth. Water infiltrates into the soil matrix during events where rainfall intensity is less than the hydraulic conductivity of the upper soil profile matrix. Even under extremely high rainfall intensity of our Experiment 2 irrigation, overland flow was not observed. Certainly, these inputs rates exceeded the soil matrix permeability, but when localized matrix infiltration rates are exceeded or when saturation of the lower portion of the soil column occurs, vertical bypass flow through visible sub-vertical cracks delivers excess water vertically to the bedrock (as shown also by McDonnell, 1990).

Our new work shows that once at the soil – bedrock interface, water flows along the bedrock surface, as evidenced by both flow routing during Experiments 1 and 2, and the observed root matting and organic staining along the soil bedrock interface during excavations. The disconnected macropore flow network perception as proposed by Weiler and McDonnell (2007) is not supported our results, since lateral macropore flow within the soil profile was not observed. Once at the soil bedrock interface, water moves either quickly downslope via a connected flowpath network of voids in the lower 5 cm of the soil profile, or leaks into the bedrock, reemerging in the vicinity of the stream channel (and below our trench collection system). High water velocities are consistent with those seen in both storm monitoring and irrigation experiments (Mosley, 1979, 1982) and a hillslope scale tracer experiment (Brammer, 1996). Leakage into bedrock at the hillslope along with reemergence at the stream channel is consistent with the low runoff ratios (on the order of 15%) observed at the hillslope (Brammer, 1996; Woods and Rowe, 1996) as compared with the high runoff ratios (on the order of 60%) seen at the first order catchment upstream (Pearce et al., 1986).

Implications on threshold for lateral subsurface flow initiation

The nature of the preferential flow network, its location and the permeability of the bedrock all have significant influence on the threshold for initiation of lateral subsurface flow. To demonstrate the influence of these factors on the threshold, we compare the findings at Maimai with another well studied field site, the Panola hillslope in Georgia, USA. Panola is similarly instrumented, with a 20 m trench collecting lateral subsurface flow from a 960 m² hillslope. At Panola, the threshold for lateral subsurface flow initiation has been attributed to the filling of subsurface storage in the small bedrock surface depressions, which occurs despite leakage into the permeable bedrock. Upslope connection of filled subsurface storage has been observed after 54 mm rainfall, coinciding with the threshold for significant lateral subsurface flow (Tromp-van Meerveld and McDonnell, 2006a,b). At the instrumented hillslope at Maimai, the threshold for flow appears to be between 17 and 23 mm of rainfall (Fig. 1).

Additional sources of the observed threshold have been proposed in previous work at the Maimai site. Pearce and Rowe (1979) estimated that canopy storage intercepted up to 3 mm rainfall at the beginning of an event. Filling of the soil moisture deficit could also account for some of the observed threshold. Soils at Maimai generally remain near field capacity throughout the year due to soil properties and the absence of an extended summer drought (Mosley, 1979). With the soils remaining wet and relatively transmissive, we do not expect that filling of the soil moisture deficit to fully account for the observed threshold, though this is the objective of a companion modeling project (Graham and McDonnell, *this issue*). These possible additional sources of the threshold do not appear to fully account for the observed 17–23 mm threshold.

The threshold for initiation of lateral subsurface flow is directly dependent on the nature of the lateral subsurface flow network. Assuming no preferential flow network (hypothesis 1a), lateral subsurface flow would initiate in the soil matrix as soon as the head gradients began to develop downslope. While this would begin soon after rainfall, with the low hydraulic conductivity of the soil matrix, substantial amounts of lateral subsurface flow would not occur until saturated conditions had spread through most of the soil profile. Assuming preferential flow was dominated by disconnected macropore flow in the soil profile (hypothesis 1b), lateral flow would not be initiated until the water table had risen above the inlet of the macropores. This flow network would need a much greater amount of precipitation to activate than the situation where there was no network at all, as the water table would

need to raise a considerable height to intersect a substantial number of macropores. Assuming the preferential flow network is a connected network at the soil bedrock interface (hypothesis 1c, supported at Maimai by these experiments), lateral subsurface flow in the preferential flow network would initiate as soon as the base of the soil profile saturated, and water began to drain into the network. Of the three available hypotheses, the connected network at the soil bedrock interface leads to the smallest threshold for significant lateral subsurface flow. At Panola, the rapid response and significant contribution of macropore flow at the soil – bedrock interface suggest that a similar flow network is occurring at Panola, and the threshold should be similar at the two sites. Since the threshold is greater at Panola, another explanation is needed.

The threshold for initiation of lateral subsurface flow is directly dependent on whether the bedrock topography controls flow routing. Assuming the bedrock surface plays an indirect role in flow routing (hypothesis 2a), the filling of bedrock topographic storage should be incidental in lateral flow generation. However, assuming the bedrock surface is the direct control of flow routing (hypothesis 2b, supported at Maimai by these experiments), topographic storage on the bedrock surface would need to be filled before lateral subsurface flow would initiate. Whereas Panola had a relatively shallow slope (14%), the hillslopes at Maimai are very steep (56%), and bedrock topographic storage volumes are likely much less at Maimai, assuming bedrock surface roughness are equal. In fact, no topographic pools larger than 1 cm deep and of diameter greater than 5 cm were observed at Maimai in the exposed bedrock surface after excavation, while apparent topographic hollows up to 8 cm deep are seen in a 1 m DEM of the Panola bedrock surface (Freer et al., 2002). The threshold for initiation of lateral subsurface flow should be greater for Panola due to the shallower slope and greater potential storage at the bedrock surface.

The threshold for initiation of lateral subsurface flow is directly dependent on the permeability of the bedrock in a system where the lateral preferential flow network is at the soil bedrock interface. Assuming a (nearly) impermeable bedrock (hypothesis 3a), bedrock topographic storage would be filled quickly, and remain filled between events. This would lead to a much lower (if any) threshold at the site. Assuming the bedrock is permeable (hypothesis 3b, supported at Maimai by these experiments), flow along the bedrock surface will drain into the bedrock while moving downslope. At the extreme case, where the bedrock permeability is equal to the permeability, no lateral subsurface flow would occur at all, as flow paths would not be diverted downslope. This case was seen at Mettmann Ridge, Oregon, where an irrigation experiment at a similarly steep forested catchment resulted in little lateral subsurface flow above the bedrock surface due to the very high permeability of the underlying fractured bedrock sandstone (Montgomery et al., 1997). In the case of Maimai, where the bedrock hydraulic conductivity (0.1–0.3 cm/h) was below the lower end of the range of the soil hydraulic conductivity (0.5 cm/h–30 cm/h), lateral subsurface flow is balanced by losses to the bedrock. The bedrock hydraulic conductivity measured at Maimai is less than that of Panola (0.58 cm/h; (Tromp-van Meerveld et al., 2006)), another possible explanation of the higher threshold (55 mm) seen at Panola.

While our work has revealed implications regarding the relative value of the threshold when compared to Panola, it is still poorly understood how each factor directly impacts the threshold at each site. Additionally, the three factors mentioned above do not encompass all possible sources of the threshold, which also include geometry of the watershed, including the percent riparian area, slope and slope length, soil textural properties such as drainable porosity and hydraulic conductivity, or environmental factors such as storm frequency and potential evaporation rates. While analysis of long term data records can help tease out environmental effects

(such as comparing the thresholds for flow for storms with different antecedent moisture conditions), determining the precise effect of geometry and bedrock and soil properties will require either extensive site intercomparison or physical and numeric modeling. Due to the wide range of factors that can potentially impact the threshold, it seems that virtual experiments are the way forward.

Conclusions

Field scale experimentation and destructive sampling demonstrated the form and function of the subsurface flow network at a well studied catchment. A hillslope excavation revealed a connected, extensive preferential lateral flow network at the soil bedrock interface capable of transmitting large volumes of water. The flow network was shown to be controlled by small scale features on the bedrock surface. Bromide tracer applications demonstrated high lateral velocities, reaching 9 m/h. A falling head test determined the bedrock was permeable, with a saturated hydraulic conductivity of 0.1–0.3 cm/h. These observations were combined with previous field observations to create a new perceptual model of flow processes at the site.

Our findings suggest that the major controls on subsurface flow paths are not the standard measured parameters, such as surface topography and soil depth, permeability and texture, but rather other, more difficult to measure parameters, such as the microscale bedrock topography, bedrock permeability, and the lateral subsurface velocities (hillslope scale anisotropy). These parameters are more difficult to measure because of their scale of operation and location, often buried beneath the soil profile. If their importance is confirmed by other studies, then new characterization methods will be needed to infer these difficult parameters on the basis of other, more easily obtained, information. Numeric models using this critical information, and perhaps simplifying less dominant processes such as transport dynamics through the soil profile, may be the key to developing new parsimonious models whose structures capture the dominant processes at a site.

Acknowledgements

This work was funded through an NSF Ecosystem Informatics internship. Chris Graham would like to thank Katherine Hoffman for providing logistical support. Tim Davie, John Payne and Jagath Ekanayake at Landcare Research provided logistical support in New Zealand. Sarah Graham, David Rupp, Gerrit Kopmann and Matt Floerl provided help with the field work.

References

- Anderson, A.E., Weiler, M., Alila, Y., Hudson, R.O., 2009. Dye staining and excavation of a lateral preferential flow network. *Hydrology and Earth System Sciences* 13 (6), 935–944.
- Atkinson, T.C., 1978. Techniques for measuring subsurface flow on hillslopes. In: Kirkby, M. (Ed.), *Hillslope Hydrology*. John Wiley & Sons, Chichester, UK, pp. 73–120.
- Bear, J., 1972. *Dynamics of Fluids in Porous Media*. American Elsevier Pub. Co., New York, p. 764.
- Brammer, D., 1996. Hillslope hydrology in a small forested catchment, Maimai, New Zealand. M.S. Thesis, State University of New York College of Environmental Science and Forestry, Syracuse, 153 pp.
- Buttle, J.M., McDonald, D.J., 2002. Coupled vertical and lateral preferential flow on a forested slope. *Water Resources Research* 38 (5).
- Flury, M., Leuenberger, J., Studer, B., Flüher, H., 1995. Transport of anions and herbicides in a loamy and a sandy field soil. *Water Resources Research* 30, 823–835.
- Freer, J. et al., 1997. Topographic controls on subsurface storm flow at the hillslope scale for two hydrologically distinct small catchments. *Hydrological Processes* 11 (9), 1347–1352.
- Freer, J. et al., 2002. The role of bedrock topography on subsurface storm flow. *Water Resources Research* 38 (12).
- Graham, C.B., McDonnell, J.J., this issue. Hillslope threshold response to rainfall: (2) development and use of a macroscale behavioral model.
- Hewlett, J.D., Hibbert, A.R., 1967. Factors affecting the response of small watersheds to precipitation in humid areas. In: Sopper, W.E., Lull, H.W. (Eds.), *Forest Hydrology*. Pergamon Press, New York, pp. 275–291.
- Hopp, L., McDonnell, J.J., 2009. Connectivity at the hillslope scale: identifying interactions between storm size, bedrock permeability, slope angle and soil depth. *Journal of Hydrology* 376, 378–391.
- Hornberger, G.M., Germann, P.F., Beven, K.J., 1991. Throughflow and solute transport in an isolated sloping soil block in a forested catchment. *Journal of Hydrology* 124, 81–99.
- Hursh, C.R., 1944. Subsurface flow. *Transactions of the American Geophysical Union* 25, 743–746.
- Hutchinson, D.G., Moore, R.D., 2000. Throughflow variability on a forested hillslope underlain by compacted glacial till. *Hydrological Processes* 14 (10), 1751–1766.
- Katsuyama, M., Ohte, N., Kabeya, N., 2005. Effects of bedrock permeability on hillslope and riparian groundwater dynamics in a weathered granite catchment. *Water Resources Research*, 41.
- Keim, R.F., Tromp-van Meerveld, H.J., McDonnell, J.J., 2006. A virtual experiment on the effects of evaporation and intensity smoothing by canopy interception on subsurface stormflow generation. *Journal of Hydrology* 327, 352–364.
- Kim, H.J., Sidle, R.C., Moore, R.D., Hudson, R., 2004. Throughflow variability during snowmelt in a forested mountain catchment, coastal British Columbia, Canada. *Hydrological Processes* 18 (7), 1219–1236.
- Kitahara, H., 1993. Characteristics of pipe flow in forested slopes. *IAHS Publication* 212, 235–242.
- Lehmann, P., Hinz, C., McGrath, G., Tromp-van Meerveld, H.J., McDonnell, J.J., 2007. Rainfall threshold for hillslope outflow: an emergent property of flow pathway connectivity. *Hydrology and Earth System Sciences* 11 (2).
- McDonnell, J.J., 1990. A rationale for old water discharge through macropores in a steep, humid catchment. *Water Resources Research* 26 (11), 2821–2832.
- McDonnell, J.J., 1997. Comment on “the changing spatial variability of subsurface flow across a hillside” by Ross Woods and Lindsay Rowe. *Journal of Hydrology (New Zealand)* 36 (1), 97–100.
- McDonnell, J.J., Owens, I.F., Stewart, M.K., 1991. A case study of shallow flow paths in a steep zero-order basin. *Water Resources Bulletin* 27 (4), 679–685.
- McDonnell, J.J. et al., 2007. Moving beyond heterogeneity and process complexity: a new vision for watershed hydrology. *Water Resources Research*, 43.
- McGlynn, B.L., McDonnell, J.J., 2003a. Quantifying the relative contributions of riparian and hillslope zones to catchment runoff. *Water Resources Research* 39 (11).
- McGlynn, B.L., McDonnell, J.J., 2003b. Role of discrete landscape units in controlling catchment dissolved organic carbon dynamics. *Water Resources Research* 39 (4).
- McGlynn, B.L., McDonnell, J.J., Brammer, D.D., 2002. A review of the evolving perceptual model of hillslope flowpaths at the Maimai catchments, New Zealand. *Journal of Hydrology* 257, 1–26.
- Montgomery, D.R. et al., 1997. Hydrologic response of a steep, unchanneled valley to natural and applied rainfall. *Water Resources Research* 33 (1), 91–109.
- Mosley, M.P., 1979. Streamflow generation in a forested watershed. *Water Resources Research* 15, 795–806.
- Mosley, M.P., 1982. Subsurface flow velocities through selected forest soils, South Island, New Zealand. *Journal of Hydrology* 55, 65–92.
- Noguchi, S., Tsuboyama, Y., Sidle, R.C., Hosoda, I., 2001. Subsurface runoff characteristics of a forest hillslope soil profile including macropores, Hitachi Ohta, Japan. *Hydrological Processes* 15, 2131–2149.
- O’Loughlin, C.L., Rowe, L.K., Pearce, A.J., 1978. Sediment yields from small forested catchments, North Westland-Nelson, New Zealand. *Journal of Hydrology (New Zealand)* 17, 1–15.
- Onda, Y., Komatsu, Y., Tsujimura, M., Fujihara, J.-i., 2001. The role of subsurface runoff through bedrock on storm flow generation. *Hydrological Processes* 15, 1693–1706.
- Pearce, A.J., Rowe, L.K., 1979. Forest management effects on interception, evaporation, and water yield. *Journal of Hydrology* 18 (2), 73–87.
- Pearce, A.J., Stewart, M.K., Sklash, M.G., 1986. Storm runoff generation in humid headwater catchments: 1. Where does the water come from? *Water Resources Research* 22, 1263–1272.
- Rowe, L.K., Pearce, A.J., O’Loughlin, C.L., 1994. Hydrology and related changes after harvesting native forests and establishing *Pinus radiata* plantations Part 1. Introduction to the study. *Hydrological Processes* 8, 263–279.
- Sidle, R.C., Hirano, T., Gomi, T., Terajima, T., 2007. Hortonian overland flow from Japanese forest plantations – an aberration, the real thing, or something in between? *Hydrological Processes* 21 (23), 3237–3247.
- Sivapalan, M., 2003. Process complexity at hillslope scale, process simplicity at the watershed scale: is there a connection? *Hydrological Processes* 17 (5), 1037–1041.
- Sklash, M.G., Stewart, M.K., Pearce, A.J., 1986. Storm runoff generation in humid headwater catchments: 2. A case study of hillslope and low-order stream response. *Water Resources Research* 22 (8), 1273–1282.
- Spence, C., Woo, M.-K., 2002. Hydrology of subarctic Canadian shield: bedrock upland. *Journal of Hydrology* 262, 111–127.
- Stewart, M.K., McDonnell, J.J., 1991. Modeling base flow soil water residence times from deuterium concentrations. *Water Resources Research* 27 (10), 2681–2693.
- Tani, M., 1997. Runoff generation processes estimated from hydrological observations on a steep forested hillslope with a thin soil layer. *Journal of Hydrology* 200, 84–109.

- Tromp-van Meerveld, H.J., McDonnell, J.J., 2006a. Threshold relations in subsurface stormflow: 1. A 147-storm analysis of the Panola hillslope. *Water Resources Research*, 42.
- Tromp-van Meerveld, H.J., McDonnell, J.J., 2006b. Threshold relations in subsurface stormflow: 2. The fill and spill hypothesis. *Water Resources Research*, 42.
- Tromp-van Meerveld, H.J., Peters, N.E., McDonnell, J.J., 2006. Effect of bedrock permeability on subsurface stormflow and the water balance of a trenched hillslope at the Panola Mountain Research Watershed, Georgia, USA. *Hydrological Processes* 21, 750–769.
- Tsuboyama, Y., Sidle, R.C., Noguchi, S., Hosoda, I., 1994. Flow and solute transport through the soil matrix and macropores of a hillslope segment. *Water Resources Research* 30 (4), 879–890.
- Uchida, T., Kosugi, K., Mizuyama, T., 1999. Runoff characteristics of pipeflow and effects of pipeflow on rainfall–runoff phenomena in a mountainous watershed. *Journal of Hydrology* 222 (1–4), 18–36.
- Uchida, T., Tromp-van Meerveld, H.J., McDonnell, J.J., 2005. The role of lateral pipe flow in hillslope runoff response: an intercomparison of non-linear hillslope response. *Journal of Hydrology* 311, 117–133.
- Waichler, S.R., Wemple, B.C., Wigmosta, M.S., 2005. Simulation of water balance and forest treatment effects at the H.J. Andrews Experimental Forest. *Hydrological Processes* 19, 3177–3199.
- Weiler, M., McDonnell, J.J., 2007. Conceptualizing lateral preferential flow and flow networks and simulating the effects on gauged and ungauged hillslopes. *Water Resources Research*, 43.
- Weiler, M., Naef, F., 2003. An experimental tracer study of the role of macropores in infiltration in grassland soils. *Hydrological Processes* 17 (2), 477–493.
- Whipkey, R.Z., 1965. Subsurface storm flow from forested slopes. *Bulletin of the International Association of Scientific Hydrology* 2, 74–85.
- Woods, R., Rowe, L., 1996. The changing spatial variability of subsurface flow across a hillside. *Journal of Hydrology (New Zealand)* 35 (1), 51–86.
- Woods, R., Rowe, L., 1997. Reply to “Comment on The changing spatial variability of subsurface flow across a hillside by Ross Woods and Lindsay Rowe”. *Journal of Hydrology (New Zealand)* 36 (1), 51–86.
- Zehe, E., Flüeler, H., 2001. Slope scale variation of flow patterns in soil profiles. *Journal of Hydrology* 247, 116–132.
- Zehe, E., Elsenbeer, H., Lindenmaier, F., K. S., Blöschl, G., 2007. Patterns of predictability in hydrological threshold systems. *Water Resources Research*, 43.